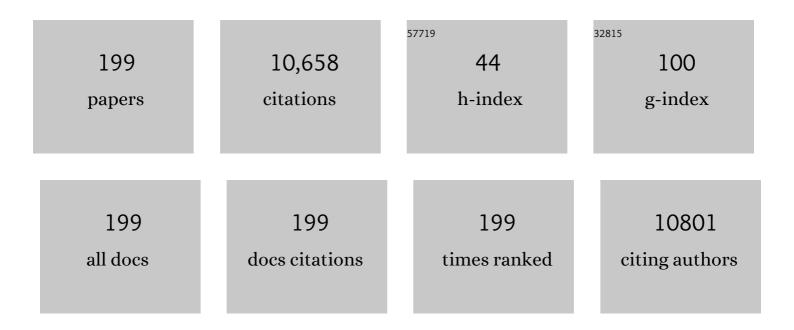
List of Publications by Year in descending order

Source: https://exaly.com/author-pdf/7625720/publications.pdf Version: 2024-02-01



RAF HO PADE

#	Article	IF	CITATIONS
1	Lanthanum-substituted bismuth titanate for use in non-volatile memories. Nature, 1999, 401, 682-684.	13.7	2,119
2	Reproducible resistance switching in polycrystalline NiO films. Applied Physics Letters, 2004, 85, 5655-5657.	1.5	890
3	Two Series Oxide Resistors Applicable to High Speed and High Density Nonvolatile Memory. Advanced Materials, 2007, 19, 3919-3923.	11.1	407
4	Electrical Manipulation of Nanofilaments in Transition-Metal Oxides for Resistance-Based Memory. Nano Letters, 2009, 9, 1476-1481.	4.5	383
5	Synthesis of Highly Crystalline and Monodisperse Cobalt Ferrite Nanocrystals. Journal of Physical Chemistry B, 2002, 106, 6831-6833.	1.2	297
6	Friction Anisotropy–Driven Domain Imaging on Exfoliated Monolayer Graphene. Science, 2011, 333, 607-610.	6.0	284
7	Interference effect on Raman spectrum of graphene on <mml:math xmlns:mml="http://www.w3.org/1998/Math/MathML" display="inline"><mml:mrow><mml:mrow><mml:mtext>SiO</mml:mtext></mml:mrow><mml:mr Physical Review B. 2009. 80</mml:mr </mml:mrow></mml:math 	ı>2 <td>nn²⁵[mml:rn</td>	nn ²⁵ [mml:rn
8	Resistive Switching Multistate Nonvolatile Memory Effects in a Single Cobalt Oxide Nanowire. Nano Letters, 2010, 10, 1359-1363.	4.5	239
9	A Low-Temperature-Grown Oxide Diode as a New Switch Element for High-Density, Nonvolatile Memories. Advanced Materials, 2007, 19, 73-76.	11.1	224
10	Differences in nature of defects between SrBi2Ta2O9 and Bi4Ti3O12. Applied Physics Letters, 1999, 74, 1907-1909.	1.5	221
11	Variations in the Raman Spectrum as a Function of the Number ofGraphene Layers. Journal of the Korean Physical Society, 2009, 55, 1299-1303.	0.3	197
12	Large Resistive Switching in Ferroelectric BiFeO ₃ Nanoâ€Island Based Switchable Diodes. Advanced Materials, 2013, 25, 2339-2343.	11.1	192
13	Effects of very thin strain layers on dielectric properties of epitaxial Ba0.6Sr0.4TiO3 films. Applied Physics Letters, 2001, 78, 533-535.	1.5	164
14	Write Current Reduction in Transition Metal Oxide Based Resistance Change Memory. Advanced Materials, 2008, 20, 924-928.	11.1	159
15	Microstructure and dielectric properties of Ba1â^'xSrxTiO3 films grown on LaAlO3 substrates. Applied Physics Letters, 2000, 77, 1200-1202.	1.5	158
16	Nanoscale Lithography on Monolayer Graphene Using Hydrogenation and Oxidation. ACS Nano, 2011, 5, 6417-6424.	7.3	138
17	Resistive-Switching Memory Effects of NiO Nanowire/Metal Junctions. Journal of the American Chemical Society, 2010, 132, 6634-6635.	6.6	125
18	Nanotribological Properties of Fluorinated, Hydrogenated, and Oxidized Graphenes. Tribology Letters, 2013, 50, 137-144.	1.2	123

#	Article	IF	CITATIONS
19	High urrentâ€Density CuO _x /InZnO _x Thinâ€Film Diodes for Crossâ€Point Memory Applications. Advanced Materials, 2008, 20, 3066-3069.	11.1	118
20	The effect of K and Na excess on the ferroelectric and piezoelectric properties of K _{0.5} Na _{0.5} NbO ₃ thin films. Journal Physics D: Applied Physics, 2009, 42, 215304.	1.3	114
21	Intrinsic Mechanisms of Memristive Switching. Nano Letters, 2011, 11, 2114-2118.	4.5	110
22	Built-in voltages and asymmetric polarization switching in Pb(Zr,Ti)O3 thin film capacitors. Applied Physics Letters, 1998, 72, 3380-3382.	1.5	108
23	High nonlinearity of Ba0.6Sr0.4TiO3 films heteroepitaxially grown on MgO substrates. Applied Physics Letters, 2000, 77, 2587-2589.	1.5	108
24	Engineering Optical and Electronic Properties of WS ₂ by Varying the Number of Layers. ACS Nano, 2015, 9, 6854-6860.	7.3	105
25	First-principles modeling of resistance switching in perovskite oxide material. Applied Physics Letters, 2006, 89, 042904.	1.5	100
26	Electrode dependence of resistance switching in polycrystalline NiO films. Applied Physics Letters, 2005, 87, 263507.	1.5	95
27	Characteristics and effects of diffused water between graphene and a SiO2 substrate. Nano Research, 2012, 5, 710-717.	5.8	91
28	Strong Polarization Dependence of Double-Resonant Raman Intensities in Graphene. Nano Letters, 2008, 8, 4270-4274.	4.5	88
29	Scaling Effect on Unipolar and Bipolar Resistive Switching of Metal Oxides. Scientific Reports, 2013, 3, 1657.	1.6	87
30	Synaptic Plasticity Selectively Activated by Polarization-Dependent Energy-Efficient Ion Migration in an Ultrathin Ferroelectric Tunnel Junction. Nano Letters, 2017, 17, 1949-1955.	4.5	79
31	Role of structural defects in the unipolar resistive switching characteristics of Ptâ^•NiOâ^•Pt structures. Applied Physics Letters, 2008, 93, .	1.5	76
32	Different fatigue behaviors of SrBi2Ta2O9 and Bi3TiTaO9 films: Role of perovskite layers. Applied Physics Letters, 1999, 75, 2644-2646.	1.5	74
33	Epitaxial Brownmillerite Oxide Thin Films for Reliable Switching Memory. ACS Applied Materials & Interfaces, 2016, 8, 7902-7911.	4.0	72
34	Ferroelectric and piezoelectric properties of Na0.52K0.48NbO3 thin films prepared by radio frequency magnetron sputtering. Applied Physics Letters, 2009, 94, .	1.5	65
35	Resistive switching transition induced by a voltage pulse in a Pt/NiO/Pt structure. Applied Physics Letters, 2010, 97, .	1.5	65
36	Decrease in switching voltage fluctuation of Ptâ^•NiOxâ^•Pt structure by process control. Applied Physics Letters, 2007, 91, 022112.	1.5	63

#	Article	IF	CITATIONS
37	Between Scylla and Charybdis: Hydrophobic Graphene-Guided Water Diffusion on Hydrophilic Substrates. Scientific Reports, 2013, 3, 2309.	1.6	60
38	Imprint failures and asymmetric electrical properties induced by thermal processes in epitaxial Bi4Ti3O12 thin films. Journal of Applied Physics, 1998, 84, 4428-4435.	1.1	59
39	Mechanical Control of Electroresistive Switching. Nano Letters, 2013, 13, 4068-4074.	4.5	55
40	Tunneling transport of mono- and few-layers magnetic van der Waals MnPS3. APL Materials, 2016, 4, .	2.2	54
41	Effects of interface charges on imprint of epitaxial Bi4Ti3O12 thin films. Applied Physics Letters, 1997, 70, 1101-1103.	1.5	52
42	Synaptic devices based on two-dimensional layered single-crystal chromium thiophosphate (CrPS4). NPG Asia Materials, 2018, 10, 23-30.	3.8	48
43	Self-renewal of embryonic stem cells through culture on nanopattern polydimethylsiloxane substrate. Biomaterials, 2012, 33, 5206-5220.	5.7	47
44	Spatial Nonuniformity in Resistive-Switching Memory Effects of NiO. Journal of the American Chemical Society, 2011, 133, 12482-12485.	6.6	46
45	Graphene/Pentacene Barristor with Ion-Gel Gate Dielectric: Flexible Ambipolar Transistor with High Mobility and On/Off Ratio. ACS Nano, 2015, 9, 7515-7522.	7.3	46
46	Resistance switching memory devices constructed on plastic with solution-processed titanium oxide. Journal of Materials Chemistry, 2009, 19, 2082.	6.7	45
47	Resistance switching in epitaxial SrCoO <i>x</i> thin films. Applied Physics Letters, 2014, 105, .	1.5	45
48	Selector-free resistive switching memory cell based on BiFeO3 nano-island showing high resistance ratio and nonlinearity factor. Scientific Reports, 2016, 6, 23299.	1.6	45
49	Dual Defects of Cation and Anion in Memristive Nonvolatile Memory of Metal Oxides. Journal of the American Chemical Society, 2012, 134, 2535-2538.	6.6	44
50	Electrically induced conducting nanochannels in an amorphous resistive switching niobium oxide film. Applied Physics Letters, 2010, 97, 233509.	1.5	42
51	Time-dependent electroforming in NiO resistive switching devices. Applied Physics Letters, 2009, 95, .	1.5	40
52	Coexistence of bi-stable memory and mono-stable threshold resistance switching phenomena in amorphous NbOx films. Applied Physics Letters, 2012, 100, .	1.5	40
53	Prominent Thermodynamical Interaction with Surroundings on Nanoscale Memristive Switching of Metal Oxides. Nano Letters, 2012, 12, 5684-5690.	4.5	40
54	Photovoltaic response and dielectric properties of epitaxial anatase-TiO2 films grown on conductive La0.5Sr0.5CoO3 electrodes. Applied Physics Letters, 2001, 79, 2797-2799.	1.5	39

#	Article	IF	CITATIONS
55	Enhanced piezoelectric properties of Ta substituted-(K0.5Na0.5)NbO3 films: A candidate for lead-free piezoelectric thin films. Journal of Alloys and Compounds, 2011, 509, L194-L198.	2.8	39
56	Brownmillerite thin films as fast ion conductors for ultimate-performance resistance switching memory. Nanoscale, 2017, 9, 10502-10510.	2.8	37
57	Study of Transport and Dielectric of Resistive Memory States in NiO Thin Film. Japanese Journal of Applied Physics, 2005, 44, L1301-L1303.	0.8	35
58	Correlative Multimodal Probing of Ionically-Mediated Electromechanical Phenomena in Simple Oxides. Scientific Reports, 2013, 3, 2924.	1.6	34
59	Enhanced Metal–Insulator Transition Performance in Scalable Vanadium Dioxide Thin Films Prepared Using a Moisture-Assisted Chemical Solution Approach. ACS Applied Materials & Interfaces, 2018, 10, 8341-8348.	4.0	34
60	Intrinsic defect-mediated conduction and resistive switching in multiferroic BiFeO3 thin films epitaxially grown on SrRuO3 bottom electrodes. Applied Physics Letters, 2016, 108, .	1.5	33
61	Segregation of oxygen vacancy at metal-HfO2 interfaces. Applied Physics Letters, 2008, 92, .	1.5	32
62	Growth Mechanism of Shape-Controlled Barium Titanate Nanostructures through Soft Chemical Reaction. Crystal Growth and Design, 2008, 8, 3180-3186.	1.4	32
63	Electrochemical growth and resistive switching of flat-surfaced and (111)-oriented Cu2O films. Applied Physics Letters, 2009, 95, 092108.	1.5	31
64	Confining grains of textured Cu2O films to single-crystal nanowires and resultant change in resistive switching characteristics. Nanoscale, 2012, 4, 2029.	2.8	31
65	Influence of the laser fluence on the electrical properties of pulsed-laser-deposited SrBi2Ta2O9 thin films. Applied Physics Letters, 1999, 75, 1155-1157.	1.5	30
66	Electrical control of nanoscale functionalization in graphene by the scanning probe technique. NPG Asia Materials, 2014, 6, e102-e102.	3.8	29
67	Mimicking a Superhydrophobic Insect Wing by Argon and Oxygen Ion Beam Treatment on Polytetrafluoroethylene Film. Journal of Bionic Engineering, 2009, 6, 365-370.	2.7	28
68	Dielectric response and structural properties of TiO2-doped Ba0.6Sr0.4TiO3 films. Applied Physics Letters, 2002, 81, 114-116.	1.5	27
69	Facile characterization of ripple domains on exfoliated graphene. Review of Scientific Instruments, 2012, 83, 073905.	0.6	27
70	Nonferroelectric epitaxial Sr–Bi–Ta oxide thin film with a high dielectric constant. Applied Physics Letters, 1998, 73, 2518-2520.	1.5	26
71	Role of atomic arrangements at interfaces on the phase control of epitaxial TiO2 films. Applied Physics Letters, 2002, 80, 1174-1176.	1.5	26
72	Synthesis of single-crystal barium titanate nanorods transformed from potassium titanate nanostructures. Materials Research Bulletin, 2008, 43, 996-1003.	2.7	26

#	Article	IF	CITATIONS
73	A Simple Device Unit Consisting of All NiO Storage and Switch Elements for Multilevel Terabit Nonvolatile Random Access Memory. ACS Applied Materials & Interfaces, 2011, 3, 4475-4479.	4.0	26
74	Growth Behavior and Electrical Properties of a (Na _{0.5} K _{0.5})NbO ₃ Thin Film Deposited on a Pt/Ti/SiO ₂ /Si Substrate Using RFMagnetron Sputtering. Journal of the American Ceramic Society, 2011, 94, 1970-1973.	1.9	26
75	Resistive switching behaviors of NiO films with controlled number of conducting filaments. Applied Physics Letters, 2011, 98, 192104.	1.5	26
76	Effect of concentration gradient on ionic current rectification in polyethyleneimine modified glass nano-pipettes. Scientific Reports, 2014, 4, 4005.	1.6	26
77	Effect of oxygen content of the LaAlO 3 layer on the synaptic behavior of Pt/LaAlO 3 /Nb-doped SrTiO 3 memristors for neuromorphic applications. Solid-State Electronics, 2018, 140, 139-143.	0.8	26
78	Giant and Stable Conductivity Switching Behaviors in ZrO2Films Deposited by Pulsed Laser Depositions. Japanese Journal of Applied Physics, 2005, 44, L345-L347.	0.8	25
79	Different nonvolatile memory effects in epitaxial Pt/PbZr0.3Ti0.7O3/LSCO heterostructures. Applied Physics Letters, 2010, 96, .	1.5	24
80	Carrier type dependence on spatial asymmetry of unipolar resistive switching of metal oxides. Applied Physics Letters, 2013, 103, .	1.5	24
81	Correlation between micrometer-scale ripple alignment and atomic-scale crystallographic orientation of monolayer graphene. Scientific Reports, 2014, 4, 7263.	1.6	21
82	Leakage Transport in the High-resistance State of a Resistive-switching NbOx Thin Film Prepared by Pulsed Laser Deposition. Journal of the Korean Physical Society, 2011, 59, 2778-2781.	0.3	21
83	Unipolar resistive switching mechanism speculated from irreversible low resistance state of Cu2O films. Applied Physics Letters, 2011, 99, 052105.	1.5	20
84	Realization of One-Diode–Type Resistive-Switching Memory with Cr–SrTiO\$_{3}\$ Film. Applied Physics Express, 2012, 5, 091202.	1.1	20
85	Switchable Schottky diode characteristics induced by electroforming process in Mn-doped ZnO thin films. Applied Physics Letters, 2013, 102, .	1.5	20
86	Nanopipette exploring nanoworld. Nano Convergence, 2014, 1, 17.	6.3	19
87	Asymmetric switching and imprint in (La,Sr)CoO3/Pb(Zr,Ti)O3/(La,Sr)CoO3 heterostructures. Integrated Ferroelectrics, 1997, 18, 39-48.	0.3	18
88	Direct investigation on conducting nanofilaments in single-crystalline Ni/NiO core/shell nanodisk arrays. Applied Physics Letters, 2010, 96, 053112.	1.5	18
89	Gate-tunable photodetector and ambipolar transistor implemented using a graphene/MoSe2 barristor. NPG Asia Materials, 2021, 13, .	3.8	18
90	Semiconductor-less vertical transistor with ION/IOFF of 106. Nature Communications, 2021, 12, 1000.	5.8	18

#	Article	IF	CITATIONS
91	Green Synthesis of Silver Nanoparticles by Sinorhizobial Octasaccharide Isolated from Sinorhizobium meliloti. Bulletin of the Korean Chemical Society, 2009, 30, 1651-1654.	1.0	18
92	Defect-related room-temperature ferroelectricity in tensile-strained SrTiO3 thin films on GdScO3 (110) substrates. Applied Physics Letters, 2010, 97, .	1.5	17
93	Memristor Behaviors of Highly Oriented Anatase TiO ₂ Film Sandwiched between Top Pt and Bottom SrRuO ₃ Electrodes. Applied Physics Express, 2011, 4, 041101.	1.1	17
94	Direct observation of potassium ions in HeLa cell with ion-selective nano-pipette probe. Journal of Applied Physics, 2012, 111, 044702.	1.1	17
95	Ferroelectric BiFeO 3 /TiO 2 nanotube heterostructures for enhanced photoelectrochemical performance. Current Applied Physics, 2017, 17, 679-683.	1.1	17
96	Universality of strain-induced anisotropic friction domains on 2D materials. NPG Asia Materials, 2018, 10, 1069-1075.	3.8	17
97	Effects of a Load Resistor on Conducting Filament Characteristics and Unipolar Resistive Switching Behaviors in a Pt/NiO/Pt Structure. IEEE Electron Device Letters, 2012, 33, 881-883.	2.2	16
98	Role of fatty acid composites in the toxicity of titanium dioxide nanoparticles used in cosmetic products. Journal of Toxicological Sciences, 2016, 41, 533-542.	0.7	16
99	Layer-to-island growth of electrodeposited Cu2O films and filamentary switching in single-channeled grain boundaries. Journal of Applied Physics, 2010, 107, .	1.1	15
100	Fabricating in-plane transistor and memory using atomic force microscope lithography towards graphene system on chip. Carbon, 2016, 96, 223-228.	5.4	14
101	Nanotribology of 2D materials and their macroscopic applications. Journal Physics D: Applied Physics, 2020, 53, 393001.	1.3	14
102	Enhanced Dielectric Properties of (Ba,Sr)TiO3Thin Tilms Applicable to Tunable Microwave Devices. Japanese Journal of Applied Physics, 2002, 41, 7222-7225.	0.8	13
103	SrFeO3 nanoparticles-dispersed SrMoO4 insulating thin films deposited from Sr2FeMoO6 target in oxygen atmosphere. Applied Physics Letters, 2004, 84, 5037-5039.	1.5	13
104	Agarose and gellan as morphology-directing agents for the preparation of selenium nanowires in water. Carbohydrate Research, 2009, 344, 260-262.	1.1	13
105	Self-separated PZT thick films with bulk-like piezoelectric and electromechanical properties. Journal of Materials Research, 2011, 26, 1431-1435.	1.2	13
106	Imaging transport current distribution in high temperature superconductors using room temperature scanning laser microscope. Review of Scientific Instruments, 2002, 73, 3692-3694.	0.6	12
107	Lead-free piezoelectric BiFeO3-BaTiO3 thin film with high Curie temperature. Current Applied Physics, 2016, 16, 1449-1452.	1.1	12
108	Large linear magnetoresistance in heavily-doped Nb:SrTiO3 epitaxial thin films. Scientific Reports, 2016, 6, 34295.	1.6	12

#	Article	IF	CITATIONS
109	Flexible resistive random access memory devices by using NiO _{<i>x</i>} /GaN microdisk arrays fabricated on graphene films. Nanotechnology, 2017, 28, 205202.	1.3	12
110	Structural Properties and Resistance-Switching Behavior of Thermally Grown NiO Thin Films. Japanese Journal of Applied Physics, 2008, 47, 1635-1638.	0.8	11
111	Synthesis of selenium nanowires morphologically directed by Shinorhizobial oligosaccharides. Carbohydrate Research, 2009, 344, 1230-1234.	1.1	11
112	Enhancement of resistive switching under confined current path distribution enabled by insertion of atomically thin defective monolayer graphene. Scientific Reports, 2015, 5, 11279.	1.6	10
113	Configuration of ripple domains and their topological defects formed under local mechanical stress on hexagonal monolayer graphene. Scientific Reports, 2015, 5, 9390.	1.6	10
114	Anteroposterior Wnt-RA Gradient Defines Adhesion and Migration Properties of Neural Progenitors in Developing Spinal Cord. Stem Cell Reports, 2020, 15, 898-911.	2.3	10
115	Fabrication and Memory Effect of Zr Nanocrystals Embedded in ZrO2Dielectric Layer. Japanese Journal of Applied Physics, 2007, 46, L1246-L1248.	0.8	9
116	The role of zinc vacancies in bipolar resistance switching of Ag/ZnO/Pt memory structures. Nanotechnology, 2012, 23, 375201.	1.3	9
117	Improved Ion-Selective Detection Method Using Nanopipette with Poly(vinyl chloride)-Based Membrane. Journal of Physical Chemistry B, 2014, 118, 5130-5134.	1.2	9
118	Real-time device-scale imaging of conducting filament dynamics in resistive switching materials. Scientific Reports, 2016, 6, 27451.	1.6	9
119	Enhanced Performance of Field-Effect Transistors Based on Black Phosphorus Channels Reduced by Galvanic Corrosion of Al Overlayers. ACS Applied Materials & Interfaces, 2018, 10, 18895-18901.	4.0	9
120	Understanding filamentary growth and rupture by Ag ion migration through single-crystalline 2D layered CrPS4. NPG Asia Materials, 2020, 12, .	3.8	9
121	Interpreting the Entire Connectivity of Individual Neurons in Micropatterned Neural Culture With an Integrated Connectome Analyzer of a Neuronal Network (iCANN). Frontiers in Neuroanatomy, 2021, 15, 746057.	0.9	9
122	Far-infrared transmission studies on a superconductingBaPb1â^'xBixO3thin film: Effects of a carrier scattering rate. Physical Review B, 1999, 59, 8869-8874.	1.1	8
123	Controlled mechnical modification of manganite surface with nanoscale resolution. Nanotechnology, 2014, 25, 475302.	1.3	8
124	High piezoelectric performance of lead-free BiFeO ₃ –BaTiO ₃ thin films grown by a pulsed laser deposition method. RSC Advances, 2016, 6, 106899-106903.	1.7	8
125	Dynamic mechanical control of local vacancies in NiO thin films. Nanotechnology, 2018, 29, 275709.	1.3	8
126	Shape-Control of Strontium Titanate Nanostructures by a Surface-Capping Soft Chemical Process. Journal of the Korean Physical Society, 2008, 52, 466-470.	0.3	8

#	Article	IF	CITATIONS
127	Separate Detection of Sodium and Potassium Ions with Sub-micropipette Probe. Japanese Journal of Applied Physics, 2011, 50, 08LB13.	0.8	8
128	The Dielectric Properties of Pb0.65Ba0.35ZrO3 Thin Films Applicable to Microwave Tunable Devices. Integrated Ferroelectrics, 2004, 66, 205-211.	0.3	7
129	Reversible Resistance Switching Behaviors of Pt/NiO/Pt Structures. Japanese Journal of Applied Physics, 2007, 46, 5205.	0.8	7
130	Separate Detection of Sodium and Potassium Ions with Sub-micropipette Probe. Japanese Journal of Applied Physics, 2011, 50, 08LB13.	0.8	7
131	Ion Current Oscillation in Glass Nanopipettes. Journal of Physical Chemistry C, 2012, 116, 14857-14862.	1.5	7
132	Enhanced piezoelectric properties of lead-free 0.935(Bi0.5Na0.5)TiO3-0.065BaTiO3 thin films fabricated by using pulsed laser deposition. Journal of the Korean Physical Society, 2013, 62, 1031-1034.	0.3	7
133	The "self spin valve―in oxygen stoichiometric SrRu 1â^'x Fe x O 3â^'î´ epitaxial thin films. Journal of Alloys and Compounds, 2016, 657, 224-230.	2.8	7
134	Progressive and Stable Synaptic Plasticity with Femtojoule Energy Consumption by the Interface Engineering of a Metal/Ferroelectric/Semiconductor. Advanced Science, 2022, 9, .	5.6	7
135	Spatial distribution analysis of critical temperature in epitaxial Y-Ba-Cu-O film using variable temperature scanning laser microscopy. IEEE Transactions on Applied Superconductivity, 2003, 13, 2894-2896.	1.1	6
136	Ferroelectricity in Ultrathin PbZrO3/PbTiO3 Artificial Superlattices by Scanning Probe Microscopy. Ferroelectrics, 2006, 336, 271-277.	0.3	6
137	Multiscale simulation on electromigration of the oxygen vacancies in metal oxides. Applied Physics A: Materials Science and Processing, 2011, 102, 909-914.	1.1	6
138	High-speed and low-voltage performance in a charge-trapping flash memory using a NiO tunnel junction. Journal Physics D: Applied Physics, 2011, 44, 155105.	1.3	6
139	Nano-domain engineering in ultrashort-period ferroelectric superlattices. Applied Physics Letters, 2012, 100, 222906.	1.5	6
140	Characterization of 12CaO·7Al ₂ O ₃ Doped Indium Tin Oxide Films for Transparent Cathode in Top-Emission Organic Light-Emitting Diodes. Journal of Nanoscience and Nanotechnology, 2013, 13, 7556-7560.	0.9	6
141	The Effect of Plasma Treatment on the Physical Properties of SrRuO3Films on SrTiO3Substrate. Journal of the Physical Society of Japan, 2013, 82, 013706.	0.7	6
142	Ultra-thin resistive switching oxide layers self-assembled by field-induced oxygen migration (FIOM) technique. Scientific Reports, 2014, 4, 6871.	1.6	6
143	Accurate and Precise Determination of Mechanical Properties of Silicon Nitride Beam Nanoelectromechanical Devices. ACS Applied Materials & Interfaces, 2017, 9, 7282-7287.	4.0	6
144	Resistive Switching Properties of a Polycrystalline TiO2 Memory Cell with a WN Buffer Layer Inserted. Journal of the Korean Physical Society, 2008, 53, 3685-3689.	0.3	6

#	Article	IF	CITATIONS
145	Nonpolar Resistance Switching in Anodic Oxide Alumina Films. Japanese Journal of Applied Physics, 2009, 48, 070207.	0.8	5
146	Electrical properties of thin films deposited with MnO- and MnO2-modified BiFeO3 oxide targets. Journal of the Korean Physical Society, 2012, 61, 1070-1074.	0.3	5
147	A new simple method for point contact Andreev reflection (PCAR) using a self-aligned atomic filament in transition-metal oxides. Nanoscale, 2015, 7, 8531-8535.	2.8	5
148	Charge-trapping memory device based on a heterostructure of MoS2 and CrPS4. Journal of the Korean Physical Society, 2021, 78, 816-821.	0.3	5
149	Unipolar Resistive Switching of EuxOy Polycrystalline Films. Journal of the Korean Physical Society, 2008, 53, 700-703.	0.3	5
150	Surface characteristics of Ni catalystic films on growth behavior of multi-walled carbon nanotubes. Applied Surface Science, 2008, 254, 4644-4649.	3.1	4
151	DIELECTRIC PROPERTIES OF EPITAXIAL Ba1-xSrxTiO3 FILMS ON MgO SUBSTRATES. Functional Materials Letters, 2011, 04, 41-44.	0.7	4
152	Selective Measurement of Calcium and Sodium Ion Conductance Using Sub-Micropipette Probes with Ion Filters. Applied Physics Express, 2012, 5, 027001.	1.1	4
153	Enhancement of the Raman scattering intensity in folded bilayer graphene. Journal of the Korean Physical Society, 2012, 60, 1278-1281.	0.3	4
154	Acceleration of Poly(L-Lactide) Degradation by TiO ₂ Nanoparticles in Sunlight. Journal of Nanoscience and Nanotechnology, 2013, 13, 6983-6987.	0.9	4
155	Effects of the fluctuation in a singly-connected conducting filament structure on the distribution of the reset parameters in unipolar resistance switching. Applied Physics Letters, 2015, 106, 133503.	1.5	4
156	Ion-Movement-Based Synaptic Device for Brain-Inspired Computing. Nanomaterials, 2022, 12, 1728.	1.9	4
157	Structure, processing, and property relationships in tunable rf and microwave devices. Integrated Ferroelectrics, 2001, 39, 261-270.	0.3	3
158	A New Candidate Material for Use in Ferroelectric Random Access Memory (Fram). Ferroelectrics, 2002, 267, 121-129.	0.3	3
159	Heteroepitaxial Growth and Ferroelectricity of Bi3.25La0.75Ti3O12Films on n-GaN/Al2O3(0001) Substrates Prepared by Pulsed-Laser Deposition. Japanese Journal of Applied Physics, 2004, 43, 7625-7626.	0.8	3
160	Ferroelectric Properties of PbZrO3/PbTiO3 Artificial Superlattices by Scanning Probe Microscopy. Integrated Ferroelectrics, 2004, 68, 13-18.	0.3	3
161	Electrostatic force microscopy study on the domain switching properties of the Pb(Zr0.2Ti0.8)O3 thin films with different crystallographic orientations for the probe-based data storage. Ultramicroscopy, 2008, 108, 1081-1085.	0.8	3
162	Magnetic phase coupled to an electric memory state in d oxide ZrO2 films. Applied Physics Letters, 2009, 95, .	1.5	3

#	Article	IF	CITATIONS
163	Development of Beetle-Type Robot with Sub-Micropipette Probe. Japanese Journal of Applied Physics, 2012, 51, 08KB12.	0.8	3
164	Ion-Selective Detection by Plasticized Poly(vinyl chloride) Membrane in Glass Nanopipette with Alternating Voltage Modulation. Journal of Nanoscience and Nanotechnology, 2013, 13, 5413-5419.	0.9	3
165	Near-band-edge photoluminescence from ZnO film: Negative thermal quenching and role of adsorbed oxygen. Journal of the Korean Physical Society, 2014, 64, 1-5.	0.3	3
166	Sample rotation angle dependence of graphene thickness measured using atomic force microscope. Carbon, 2015, 81, 210-215.	5.4	3
167	Direct Observation of Domain Motion Synchronized with Resistive Switching in Multiferroic Thin Films. ACS Applied Materials & amp; Interfaces, 2016, 8, 35464-35471.	4.0	3
168	Influence of Mn-oxide Nanoclusters on the Electric Properties ofZnO:Mn Films. Journal of the Korean Physical Society, 2009, 55, 20-23.	0.3	3
169	Pulsed laser deposition of Bi4Ti3O12 thin films and their anomalous imprint characteristics. Integrated Ferroelectrics, 1997, 14, 181-191.	0.3	2
170	Deposition of SrFeO3â^'Î-Dispersed SrMoO4 Oxide Thin Films on Si (100) Surface for Spintronic Applications. Integrated Ferroelectrics, 2004, 67, 25-30.	0.3	2
171	Dynamics of resistance switching induced by charge carrier fluence. Journal of Applied Physics, 2010, 108, 074101.	1.1	2
172	EFFECTS OF ARGON+ ION BOMBARDMENT ON A PLATINUM/ZIRCONIUM DIOXIDE/IRIDIUM RESISTIVE SWITCHING MEMORY CELL. Functional Materials Letters, 2011, 04, 71-74.	0.7	2
173	Correlation between Resistance Switching States and Photoluminescence Emission in ZnO Films. Applied Physics Express, 2011, 4, 075801.	1.1	2
174	Detection of Single Nucleotide Polymorphisms Using a Biosensor-Containing Titanium-Well Array. Journal of Nanoscience and Nanotechnology, 2013, 13, 139-143.	0.9	2
175	Reduced distributions of the set current and the voltage of unipolar resistance switching in a current-biased set process. Journal of the Korean Physical Society, 2016, 68, 1467-1471.	0.3	2
176	Strain Mismatch Induced Tilted Heteroepitaxial (000 <i>l</i>) Hexagonal ZnO Films on (001) Cubic Substrates. Advanced Engineering Materials, 2011, 13, 1142-1145.	1.6	1
177	Investigation of vertically trapped charge locations in Cr-doped-SrTiO3-based charge trapping memory devices. Journal of Applied Physics, 2012, 112, 074505.	1.1	1
178	Thickness-dependent resistance switching in Cr-doped SrTiO3. Journal of the Korean Physical Society, 2012, 61, 754-758.	0.3	1
179	Reversible quenching of luminescence in ZnO films by electric field action. Physica Status Solidi - Rapid Research Letters, 2015, 9, 307-311.	1.2	1
180	Large Temperature-Independent Magnetoresistance without Gating Operation in Monolayer Graphene. ACS Applied Materials & Interfaces, 2020, 12, 53134-53140.	4.0	1

#	Article	IF	CITATIONS
181	Electrical Properties of MoS2 Field-Effect Transistors in Contact with Layered CrPS4. Journal of the Korean Physical Society, 2020, 76, 731-735.	0.3	1
182	Ripples, Wrinkles, and Crumples in Folded Graphene. Journal of the Korean Physical Society, 2020, 76, 985-990.	0.3	1
183	Temperature dependence of tunneling current in Pt/Nb:SrTiO3 Schottky junction. Applied Physics Letters, 2020, 116, 022901.	1.5	1
184	NANO-PIPETTE PROBE WITH SEPARATIVE ION DETECTION. , 2011, , .		1
185	Effects of the Crystalline Properties on the Dielectric Performances in Ba0.5Sr0.5TiO3 Thin Films. Journal of the Korean Physical Society, 2008, 52, 421-426.	0.3	1
186	Development of Beetle-Type Robot with Sub-Micropipette Probe. Japanese Journal of Applied Physics, 2012, 51, 08KB12.	0.8	1
187	Engineering ferromagnetic lines in graphene by local oxidation and hydrogenation using nanoscale lithography. Journal Physics D: Applied Physics, 2021, 54, 074002.	1.3	1
188	Dielectric properties of Ba0.6Sr0.4TiO3 thin films with various strain states. Integrated Ferroelectrics, 2001, 39, 271-280.	0.3	0
189	Investigation on Resistive Memory Switching Mechanism of NiO. Integrated Ferroelectrics, 2007, 93, 90-97.	0.3	0
190	BaTiO3 Doped Na0.5K0.5NbO3 Thin Films Deposited by Using Eclipse Shutter Enhanced Pulsed Laser Deposition Method. Journal of Nanoscience and Nanotechnology, 2009, 9, 7354-8.	0.9	0
191	Raman Spectroscopy of Graphene (abstract). , 2009, , .		0
192	Resistance States and Photoluminescence in Anodic Oxide Alumina Films. Electrochemical and Solid-State Letters, 2009, 12, G47.	2.2	0
193	Influence of MnO clusters on resistance switching behaviors in ZnO/n-Si structures. Journal of the Korean Physical Society, 2012, 60, 1531-1534.	0.3	0
194	Kinetics of nanodomain growth in ferroelectric artificial superlattices. Scripta Materialia, 2013, 69, 501-504.	2.6	0
195	Effect of A-site Excess on the Piezoelectric Properties of (K _{0.48} Na _{0.52}) _{1+<i>x</i>} (Nb _{0.55} Ta _{0.45})O <su Films. Ferroelectrics, 2014, 465, 60-67.</su 	ıbx & s/sul	o>T b in
196	Effects of near-surface defects on the optical, electrical and magnetic properties of ZnO films. Journal of the Korean Physical Society, 2014, 64, 1590-1594.	0.3	0
197	Carrier Transport Properties of Bilayer Graphene Obtained via Hall Measurements. Journal of Nanoscience and Nanotechnology, 2015, 15, 7482-7485.	0.9	0
198	Physical Issues and Applications of Resistive Switching Phenomena. Journal of the Korean Physical Society, 2018, 73, 852-857.	0.3	0

#	Article	IF	CITATIONS
199	FABRICATION OF GRAPHENE OXIDE USING LOCAL ANODIC OXIDATION BY ATOMIC FORCE MICROSCOPY. , 2011, , .		0